Physiologia Plantarum
An International Journal for Plant Biology

Anatomical and hormonal description of rootlet primordium development along white lupin cluster root

Cécilia Gallardo†, Bárbara Hufnagel†, Célia Casset, Carine Alcon, Fanny Garcia, Fanchon Divol, Laurence Marquès, Patrick Doumas and Benjamin Péret*

BPMP, University of Montpellier, CNRS, INRA, SupAgro, Montpellier, France

Correspondence
*Corresponding author,
e-mail: benjamin.peret@cnrs.fr

Received 18 December 2017;
revised 26 February 2018

doi:10.1111/ppl.12714

Cluster root (CR) is one of the most spectacular plant developmental adaptations to hostile environment. It can be found in a few species from a dozen botanical families, including white lupin (*Lupinus albus*) in the Fabaceae family. These amazing structures are produced in phosphate-deprived conditions and are made of hundreds of short roots also known as rootlets. White lupin is the only crop bearing CRs and is considered as the model species for CR studies. However, little information is available on CRs atypical development, including the molecular events that trigger their formation. To provide insights on CR formation, we performed an anatomical and cellular description of rootlet development in white lupin. Starting with a classic histological approach, we described rootlet primordium development and defined eight developmental stages from rootlet initiation to their emergence. Due to the major role of hormones in the developmental program of root system, we next focussed on auxin-related mechanisms. We observed the establishment of an auxin maximum through rootlet development in transgenic roots expressing the *DR5:GUS* auxin reporter. Expression analysis of the main auxin-related genes [TIR, Auxin Response Factor (ARF) and AUX/IAA] during a detailed time course revealed specific expression associated with the formation of the rootlet primordium. We showed that *L. albus TRANSPORT INHIBITOR RESPONSE 1b* is expressed during rootlet primordium formation and that *L. albus AUXIN RESPONSE FACTOR 5* is expressed in the vasculature but absent in the primordium itself. Altogether, our results describe the very early cellular events leading to CR formation and reveal some of the auxin-related mechanisms.

Introduction

Cluster roots (CRs) or proteoid roots are specific organs that are produced by the Proteaceae and a limited number of species belonging to several botanical families that are adapted to habitats with extremely low soil fertility (Shane and Lambers 2005, Lambers et al. 2015). Indeed, CRs correspond to peculiar lateral roots (LRs) producing bottlebrush-like clusters of short rootlets (reviewed in Vance et al. 2003; Fig. 1A, B). These organs represent an evolutionary adaptation to phosphorus-impoverished soils. As a result, CRs exhibit four main characteristics regarding their development and physiology (Skene

Abbreviations – AuxREs, auxin response elements; ARF, auxin response factor; AUX/LAX, AUXIN RESISTANT–LIKE-AUX1; CR, cluster root; GUS, ß-glucuronidase; LR, lateral root; Pi, inorganic phosphate; PIN, PIN FORMED; SCF, SKP-Cullin F-box; *LaARF5*, *Lupinus albus AUXIN RESPONSE FACTOR 5*; *LaTIR1b*, *Lupinus albus TRANSPORT INHIBITOR RESPONSE 1b*.

†These authors equally contributed to this work.

2000): (1) a massive induction of rootlets (up to 20–100 per cm); (2) a determinate development leading to a limited growth and subsequent entry into senescence; (3) an exudative burst resulting in massive secretion of protons, organic acids, phenolics and phosphate remobilizing enzymes and (4) a high phosphate uptake capacity. The secretion of protons can be imaged with a pH indicator such as bromocresol purple (Fig. 1C). A high level of ferric reductase activity is also associated with CR physiology and can be revealed biochemically (Fig. 1D).

White lupin (*Lupinus albus*) is an annual legume traditionally cultivated around the Mediterranean and is also the only cultivated crop that can form CRs. It is a model of interest because of its quick life cycle compared to other species, mainly bushes and trees, sharing the ability to form these structures. Moreover, white lupin has the capacity to form nitrogen-fixing nodules as a result of the symbiotic interaction with *Bradyrhizobium sp*. but has lost the ability to form mycorrhizal associations (Lambers and Teste 2013). Interestingly, many CR forming species share this lack of ability for mycorrhization. The capacity to form CRs in lupin allows a reduction of phosphate fertiliser use in the field and results in a beneficial interaction in mixed cultures (Cu et al. 2005); this represents an interesting example to lower our dependency on this source of agricultural input.

In this study, we used white lupin CR as a model to study a highly exacerbated mode of LR initiation and development. Indeed, production of numerous rootlets means that several sites of LR formation are activated in an almost synchronous manner (Hagström et al. 2001). Regular LR development involves several fundamental mechanisms that have been largely described, including in the model plant *Arabidopsis thaliana*. LR formation starts early in the primary root apex where pre-branching sites are defined (Moreno-Risueno et al. 2010, Xuan et al. 2015). Later on, founder cell specification occurs in the pericycle to trigger the initiation event (Dubrovsky et al. 2008, De Rybel et al. 2010). The LR primordium then undergoes a series of divisions following a defined pattern (Malamy and Benfey 1997) and simultaneously emerges through the outer tissues to reach the rhizosphere (Laskowski et al. 2006). This developmental process is thought to be iterative for higher order LRs but very few studies have focussed on this subsequent step. In lupin, we can imagine that these fundamental mechanisms are amplified to produce hundreds of rootlets. It is therefore possible to learn more about the regulatory mechanisms of LR development by studying lupin CR development.

It is well known that several hormones control LR formation (Fukaki and Tasaka 2009), among which auxin acts as a positive regulator (Du and Scheres 2017) whereas cytokinins have a negative impact (Laplaze et al. 2007). Auxin transport is polar and achieved by various transporters including PIN (PIN FORMED) efflux and AUX/LAX (AUXIN RESISTANT–LIKE-AUX1) influx carriers (Benková et al. 2003, Billou et al. 2005). Auxin regulates the transcriptional activity of several

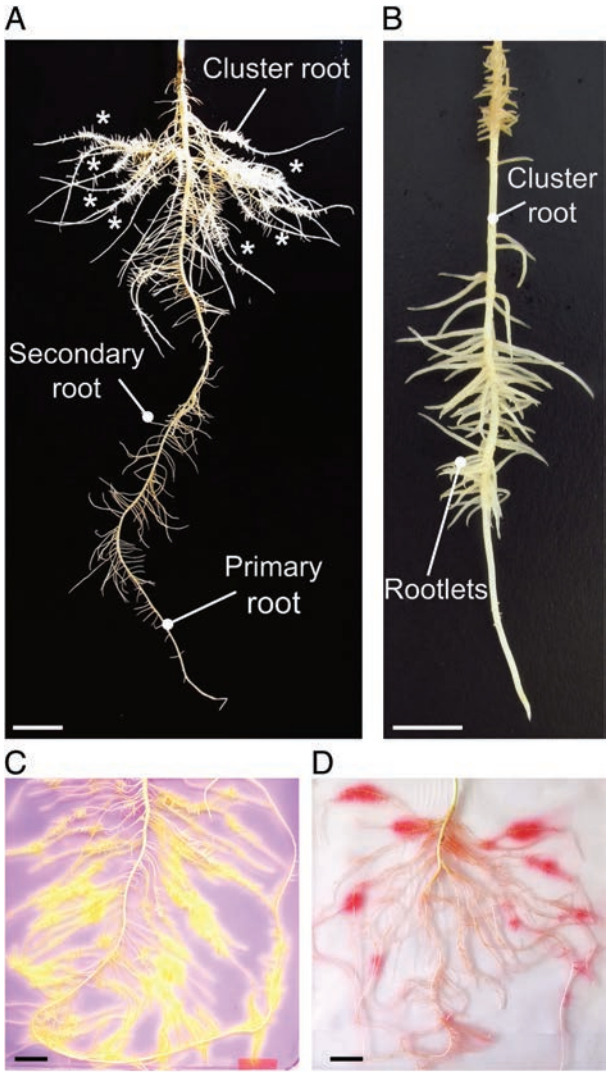

Fig. 1. White lupin architecture and physiology in low phosphate conditions. (A and B) Root architecture of a 21-day-old white lupin (*Lupinus albus*) comprising many CRs in the upper part of the root system (asterisks). CRs are secondary roots producing hundreds of short roots with determinate development, known as rootlets (B). (C and D) Physiological assays of 19-day-old lupin root systems placed on agar plates containing bromocresol purple (BCP) (C) or bathophenanthroline disulfonic acid disodium salt (BPDS) in the presence of Na-Fe EDTA (D). (C) BCP is a purple pH indicator that turns yellow when the roots are acidifying the medium with proton excretion (pH < 5). (D) BPDS allow visualisation of ferric reductase activity upon reduction of Fe^{3+} to Fe^{2+}, with appearance of a pink coloration. Scale bars are 2.5 cm (A, C, D) and 0.5 cm (B).

genes through the action of the $SCF^{TIR/AFB}$ complex, which comprises TIR1 auxin receptor (F-box protein) (Dharmasiri et al. 2005, Kepinski and Leyser 2005) and a SCF (SKP-Cullin F-box) type ubiquitin E3 ligase. Together with the Aux/IAA repressor, they form the auxin receptor complex. In the presence of the ligand, the complex tags Aux/IAA for degradation, therefore releasing the auxin response factor (ARF) proteins. ARF proteins are known to regulate (activate or repress) transcription by binding to specific auxin response elements (AuxREs) in the target gene promoter (Ulmasov et al. 1997, Ulmasov et al. 1999). In fact, the establishment of a meristem is always accompanied by the establishment of an auxin maximum (Benková et al. 2003). Such auxin gradient has not yet been described in white lupin rootlets. Previous studies reported the accumulation of auxin in lupin roots as a response to low phosphate conditions (Meng et al. 2013). Accordingly, exogenous auxin treatments favour the formation of numerous roots but whether they are CRs has not been formally demonstrated (Meng et al. 2013). The expression of various auxin-related genes (transport, synthesis) has been reported but no detailed expression patterns have been shown (Wang et al. 2014, Wang et al. 2015). Given the determinate nature of rootlet meristems, the establishment of an auxin gradient may be transitory or not even happen.

In this study, we focussed on rootlet development because it represents an optimal model for LR development for two major reasons: (1) rootlets are massively and synchronously induced in phosphate starvation conditions and (2) rootlets have a determinate development. We achieved a histological description of rootlet development during CR formation in white lupin to describe the early cellular division events. We demonstrated the establishment of an auxin gradient during rootlet primordia formation by studying the *DR5:GUS* marker in white lupin. We set up a time course sampling approach to dissect auxin-related gene expression and focussed on two genes. Cloning *L. albus TRANSPORT INHIBITOR RESPONSE 1b* (*LaTIR1b*) and *L. albus AUXIN RESPONSE FACTOR 5* (*LaARF5*) promoters allowed us to determine their expression pattern during rootlet development and to validate an important role of auxin during this process.

Materials and methods

Plant materials and growth conditions

Seeds of white lupin (*L. albus* cultivar Amiga obtained from Florimond Desprez, France) were used in all experiments. Seeds were germinated on vermiculite substrate for 4 days. Seedlings were cultivated in growth chambers under controlled conditions (16 h light/8 h dark, 25°C day/20°C night, 65% relative humidity and PAR intensity 200 $\mu mol\, m^{-2}\, s^{-1}$). After germination, four seedlings were transferred to 1.6-l pots. The hydroponic solution was modified from (Abdolzadeh et al. 2010) without phosphate, according to the following composition: $MgSO_4$, 54 µM; $Ca(NO_3)_2$ 400 µM; K_2SO_4 200 µM; Na-Fe-EDTA 10 µM; H_3BO_3 2.4 µM; $MnSO_4$ 0.24 µM; $ZnSO_4$ 0.1 µM; $CuSO_4$ 0.018 µM and Na_2MoO_4 0.03 µM. The nutrient solution was continuously aerated and was renewed every 7 days.

CR physiological assays

For all functional assays, the roots of 3-week-old plants were thoroughly washed in ultra pure water, and carefully pressed on agar sheets to avoid damaging the roots and covered with a transparent film. For visualisation of protons excretion, agar sheets contained: 0.8% agar (w/v), 0.005% bromocresol purple buffered with Tris–HCl 1 mM pH 6, 2 mM K_2SO_4 and 1 mM $CaSO_4$. For visualisation of ferric reductase activity, agar sheets were prepared as follows: 0.8% agar (w/v), 100 µM Na-Fe-EDTA, 300 µM bathophenanthroline disulfonic acid and 1 mM K_2SO_4. Agar plates were allowed to set at room temperature for 6 h in the dark.

Low coverage genome sequencing

To generate a genomic dataset of white lupin, DNA from leaf tissue was extracted using Qiagen Genomic-tip 100 according to the manufacturer's protocol (Qiagen, Hilden, Germany). The integrity and quality of total DNA were checked using NanoDrop 1000 Spectrophotometer (Thermo Fisher, Waltham, MA) and formaldehyde agarose gel electrophoresis, and DNA was quantified using a Qubit fluorometer (Promega, Madison, WI). Short-reads sequencing (150 bp) was performed using the Illumina Hiseq 3000 platform at GenoToul (Toulouse, France), generating 79 424 562 reads. Quality assessment and trimming of the reads were performed with FastQC (http://www.bioinformatics.babraham.ac.uk/projects/fastqc) and the FASTX-Toolkit (http://hannonlab.cshl.edu/fastx_toolkit/index.html), respectively.

In silico genome walking

In order to identify the promoter sequences of *LaTIR1b* (LAGI02_15246) and *LaARF5* (LAGI02_2355) whose cDNA were obtained from the white lupin gene index (LAGI02) previously published (Secco et al. 2014), we set up a technique that we named in silico genome walking (ISGW). ISGW is achieved in two steps: (1) the Illumina reads are mapped against a cDNA sequence from the

gene of interest (reference sequence) using BBmap v. 37.41 (https://sourceforge.net/projects/bbmap/) and (2) all mapping reads are assembled into a slightly larger contig using CAP3 (Huang and Madan 1999). The process is repeated by using the larger contig as a reference for a next round of assembly, therefore initiating the genome walking process (both ways). ISGW was performed until we obtained contigs containing 1000 bp upstream of the ATG start codon. This sequence information was then used to clone the promoter by PCR amplification.

Molecular cloning

The primers for *pLaTIR1b* (F-5′-TCATTTCCAAACTTATAAGTGG-3′; R-5′-GGTCGTTGATTCACTGATGAAACG-3′) and *pLaARF5* (F-5′-GATCCTTTTAGAGAGTTGG-3′; R-5′-GCAACACCATCAAATTCAATAAG-3′) were designed using Primer3Plus (Untergasser et al. 2012). They were used to amplify a total of 986 and 898 bp upstream of the start codon of *LaTIR1b* and *LaARF5*, respectively, from white lupin genomic DNA with the addition of the attb1 (5′-GGGGCCAAGTTTGTACAAAAAAGCAGGCT-3′) and attb2 (5′-CCCCCCACTTTGTACAAGAAAGCTGGGT-3′) adapters. Amplified fragments were subsequently cloned into the pDONR221 by Gateway reaction (Thermo Fisher). The promoters were then cloned into the binary plasmid pKGW-FS7 (Karimi et al. 2002) containing a green fluorescent protein - glucuronidase (GFP-GUS) fusion by Gateway cloning.

Bacterial strain

Agrobacterium rhizogenes strain *ARqual* was used to perform 'hairy root' transformation of white lupin. Bacteria were transformed with the binary plasmid by electroporation and confirmed by PCR and sequencing. LB agar plates (agar 0.8%) added with acetosyringone 100 µM were inoculated with 200 µl of liquid bacteria culture and incubated at 28°C for 24 h to get a bacterial lawn. Bacterial lawn was used for white lupin seedling transformation.

Hairy root transformation of white lupin

White lupin seedlings were transformed following protocol previously described (Uhde-Stone et al. 2005). White lupin seeds were surface sterilised by four washes in osmosed water, 30 min sterilisation in bleach (Halonet 20%, Proquimia, Barcelona, Spain) and washed six times in sterile water. Seeds were germinated in the dark in water. After germination, radicles of 1 cm were cut over 0.5 cm with a sterile scalpel. The radicles were inoculated with the *A. rhizogenes* culture. Fifteen inoculated seedlings were placed on square agar plates (0.7% agar in 1× Hoagland solution) containing 15 µg ml^{-1} kanamycin. Plates were placed vertically in growth chambers (Fitotron, Weiss Technik, Eragny, France) in controlled conditions: 18 h light/6 h dark, at 25°C, 60% relative humidity with a PAR intensity of about 130 µmol m^{-2} s^{-1}. Seedlings were transferred to fresh plates every 7 days for 3 weeks after germination. Timentin (150 µg ml^{-1}) was added to the agar medium after 1 week on plates to limit bacterial growth. Plants growing 'hairy roots' were transferred after 3 weeks in 1.6-l pot containing nutrient solution with 15 µg ml^{-1} timentin. Nutrient medium was renewed each week. After 7 days in hydroponic conditions, CRs were sampled on 'hairy root' plants. Each root represents an independent transformation event and we observed n = 89 roots from *DR5:GUS* plants, n = 47 roots from *pTIR1b:GUS* plants and n = 26 roots from *pARF5:GUS* plants.

Histochemical analysis

Histochemical staining of *β*-glucuronidase was performed on CRs from 'hairy root' plants. Samples were incubated in a phosphate buffer containing 1 mg ml^{-1} X-Gluc as a substrate (X-Gluc 0.1%; phosphate buffer 50 mM, pH 7, potassium ferricyanide 2 mM, potassium ferrocyanide 2 mM, Triton X-100 0.05%). Coloration was performed as follows: 2 h incubations for *pDR5:GUS*, 30 min incubation for *pLaTIR1b:GFP-GUS* or 2.5 h for *pLaARF5:GFP-GUS*. Tissues were fixed in a 2% formaldehyde/1% glutaraldehyde/1% caffeine solution in a phosphate buffer at pH 7. Tissues were fixed for 2.5 h under shaking at room temperature and then 1.5 h at 4°C.

Microscopic analysis

For thin section, roots were dehydrated in successive ethanol solutions with increased concentrations: 50% (30 min), 70% (30 min), 90% (1 h), 95% (1 h), 100% (1 h) and 100% (overnight). Samples were impregnated with 50% pure ethanol and 50% resin (v/v), then in 100% resin. CRs were embedded in Technovit 7100 resin (Heraeus Kulzer, Wehrheim, Germany) according to the manufacturer's recommendations. For thick sections of 80 µm, CRs were embedded in agarose 4% (m/v) and cut with a vibratome (Microcut H1200, Bio Rad, Hercules, CA). The whole mount root tissues were cleared with 0.1% ClearSee (Kurihara et al. 2015) in phosphate buffer saline (PBS) 1X solution and mounted

on slides in water. Thin sections of 6 µm were produced using a microtome (RM2165, Leica Microsystems, Wetzlar, Germany). They were counterstained for 5 min either with 0.05% toluidine blue or with 0.1% ruthenium red in a phosphate buffer (pH 7.4). All sections were observed with a colour camera on Olympus BX61 epifluorescence microscope (Tokyo, Japan) with Camera ProgRes®C5 Jenoptik and controlled by ProgRes Capture software (Jenoptik, Jena, Germany).

Expression analysis

A total of eight CRs coming from four independently grown plants were sampled 7 days after germination every 12 h. Total RNA from these samples was extracted using the Direct-zol RNA MiniPrep kit (Zymo Research, Irvine, CA) according to the manufacturer's recommendations. RNA concentration was measured on a NanoDrop (ND1000) spectrophotometer. Poly(dT) cDNA were prepared from 1.5 µg total RNA using the revertaid First Strand cDNA Synthesis (Thermo Fisher). Gene expression was measured by quantitative Real Time - Polymerase Chain Reaction (qRT-PCR) (LightCycler 480, Roche Diagnostics, Basel, Switzerland) using the SYBR Premix Ex Taq (Tli RNaseH, Takara, Clontech, Mountain View, CA) in 384-well plates (Dutscher, Brumath, France). Target quantifications were performed with specific primer pairs designed using Universal Probe Library software (Roche Diagnostics, Basel, Switzerland). The two primer pairs used in the parallel PCR reaction were: *LaTIR1b* F-5′-AACCTACTACGTTGGTGTCCTCA-3′ and *LaTIR1b* R-5′-CTCTGTCGAGCAGACTCCTGT-3′; *LaARF5* F-5′-GACGATGAAAATGACATGATGC-3′ and *LaARF5* R-5′-AATAATACAGAATTCCGGCCATC-3′. Expression level was normalised to *LaUBIQUTIN* (*LaUBQ*). The primer pairs used were *LaUBQ* F-5′-ATGTCAAAGCCAAGATCCAAG-3′ and R-5′-GAACCTTCCCAGAATCATCAA-3′ (Meng et al. 2012). All qRT-PCR experiments were performed in technical quadruplicates and the values presented represent means ± SD. Relative gene expression levels were calculated according to the ΔΔCt method (Livak and Schmittgen 2001). All experiments were performed as four biological replicates.

Results

Characterisation of rootlet primordium development in white lupin

If the cellular events leading to the formation of LRs have been well described (Malamy and Benfey 1997, Casimiro et al. 2003, Péret et al. 2009, Von Wangenheim et al. 2016), especially in the model plant *A. thaliana*, little information is available about the contribution of root tissues to CR development, especially in white lupin. To describe CR development, our aim was first to provide a tissular description of rootlet primordia development. To achieve this objective, we generated thin cross sections of 14-day-old CRs that were subsequently stained with toluidine blue to reveal the cell layers. Lupin roots comprise only one layer of pericycle, endodermis and epidermis as well as five to six layers of cortical cells (Fig. 2A, B). Observation of these thin sections by photonic microscopy allowed the observation of the early cellular events throughout the course of rootlet development. By analogy with LR development in the model plant Arabidopsis, we defined eight developmental stages from initiation (stage I) to emergence (stage VIII), as shown in Fig. 2 and described below.

On the cross sections, the earliest visible event of rootlet formation corresponded to a periclinal division in the pericycle close to a protoxylem pole (stage Ia, Fig. 2C, black arrow). This division was followed by a second periclinal division in the pericycle cells (stage Ib, Fig. 2D, black arrows). At stage II, it seemed that pericycle cells continued to divide periclinally as more cell walls were observed in these cells. These divisions gave birth to two pericycle layers: P1 and P2. Approximately at the same moment, periclinal divisions were also observed in the endodermis tissue, overlaying the pericycle cells (stage II, Fig. 2E, black arrow). As a consequence, we observed a rootlet primordium with four layers (P1, P2, E1 and E2) that was about ten cells in length (stage II, Fig. 2E). A first radial division was also seen in the pericycle at the lateral primordium boundary (stage II, Fig. 2E, purple arrow). The following stage was characterised by further periclinal divisions in the pericycle and endodermis tissues (stage III, Fig. 2F, purple arrows). Cell divisions in the next following stages became more and more difficult to characterise as the primordium was increasing both in length and width. Numerous cells continued to divide, giving progressively birth to a typical dome shaped primordium. At stage IV, rootlet primordium development coincided with intensive cell divisions happening between the xylem pole and the P1 pericycle tissue in the procambial tissue (stage IV, Fig. 2G, black arrow). A radial division was seen in the overlaying cortical tissue, suggesting a possible role of cortex tissue in rootlet primordium development (stage IV, Fig. 2G, purple arrow). Stage V of rootlet primordium development coincided with further divisions in the procambial tissue and at the apex of rootlet primordium (stage V, Fig. 2H, black arrow). Lens-shaped cells also appeared at the edges of rootlet primordium (stage V, Fig. 2H,

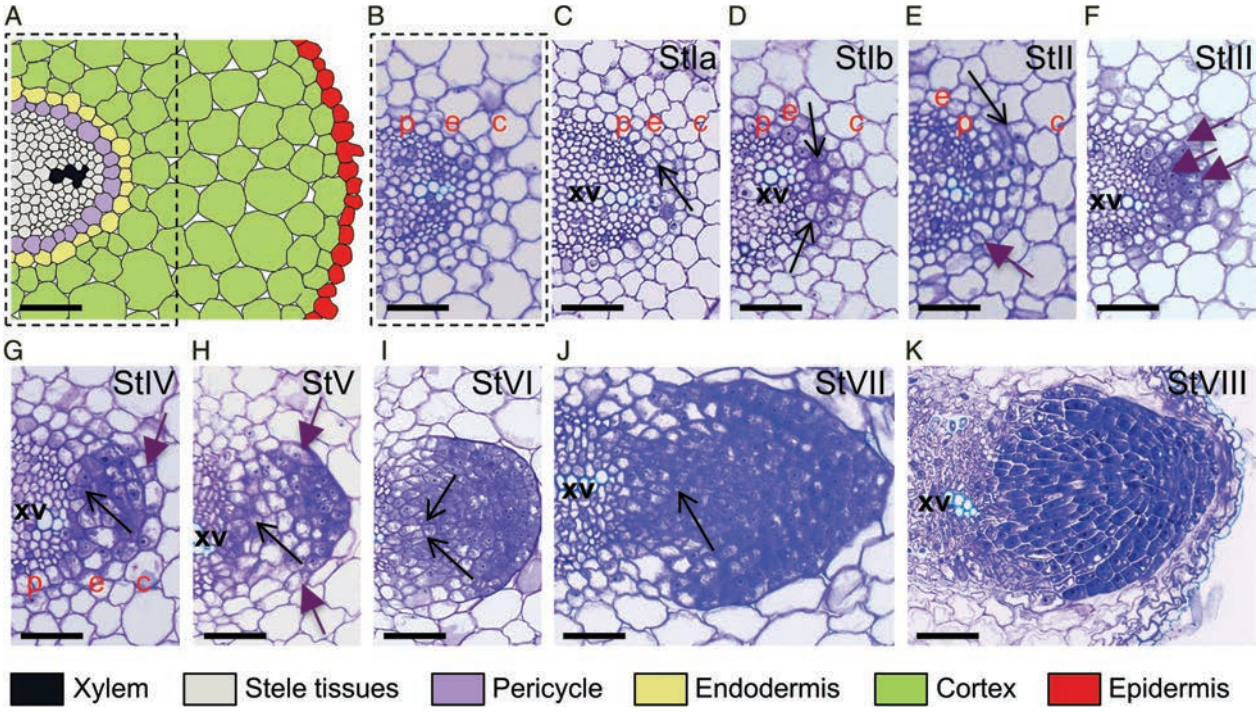

Fig. 2. Rootlet primordium development during CR formation in white lupin. Radial cellular organisation of white lupin CR (A) drawn from a thin cross section of CR from 24-day-old P-deficient plants (B). Xylem vessel elements are stained in blue and non-lignified cells walls are stained in purple by toluidine blue. (C) A first periclinal division is seen in the pericycle at stage Ia. (D) A second cell is dividing in the pericycle (stage Ib). (E) Periclinal divisions are occurring in the endodermis (stage II). (F) Numerous anticlinal divisions are seen in the pericycle and endodermis tissues (stage III). (G) More cell divisions in the pericycle and endodermis give rise to a dome-shaped rootlet primordium that is about to cross cortex and several cells are dividing at the base of the primordium between the pericycle and protoxylem pole (stage IV). (H) Cells are proliferating at the base and the apex of the primordium (stage V). (I) Primordium has crossed half of the cortex and some elongated cells are appearing in the centre of the primordium (stage VI). (J) The rootlet primordium is made of numerous cells and is about to reach the epidermis of the secondary root. Note the deformation of the cortex occurring when rootlet is about to emerge (stage VII). (K) The new primordium is crossing the epidermal layer and reaching the rhizosphere (stage VIII). p, pericycle; e, endodermis; c, cortex; xv, xylem vessels. Scale bars are 50 µm.

purple arrows). In the next stage of rootlet development, stage VI, rootlet primordium had crossed half of the main CR and was much larger. This progression through the outer tissues caused the surrounding cortical cells to be distorted and displaced (stage VI, Fig. 2I). At this stage, elongated cells could be observed in the centre of the rootlet primordium, reminiscent of vascular elements (stage VI, Fig. 2I, black arrows). A core of cells at the apex gave rise to a croissant-shaped structure that looks like a typical root cap at the tip of the rootlet primordium (stage VI, Fig. 2I). From this stage onwards, new cell divisions were really difficult to characterise due to the high number of cells and their small volume. At stage VII, the primordium was crossing the last layers of cortical cells of the main CR and was about to emerge in the surrounding rhizosphere. At this stage, an important number of elongated cells were visible in the centre of the rootlet primordium and seemingly connected to the vasculature of the main CR (stage VII, Fig. 2J, black arrow). Primordia grew from 70 µm in width and 115 µm in length at stage IV (Fig. 2G) to 180 µm in width and 220 µm in length at stage VIII (Fig. 2K). When the rootlet was about to emerge, the primordium was more than four times longer than Arabidopsis LR primordium, which is typically about 50 µm in length. In the last step, stage VIII, the new formed rootlet was crossing the epidermis and emerging (stage VIII, Fig. 2K).

Establishment of an auxin gradient during rootlet morphogenesis

The major role of auxin during LR development has been described into great detail (Lavenus et al. 2013), notably with the help of the synthetic auxin reporter DR5 (Ulmasov et al. 1997). We generated white lupin composite transgenic 'hairy root' plants expressing the DR5 reporter fused to the ß-glucuronidase gene. Our first goal was to determine whether the 'hairy root' system is suitable to observe auxin-related developmental mechanisms and subsequently to determine whether an auxin gradient is established during rootlet organogenesis. In white lupin, the DR5 marker, an artificial promoter made

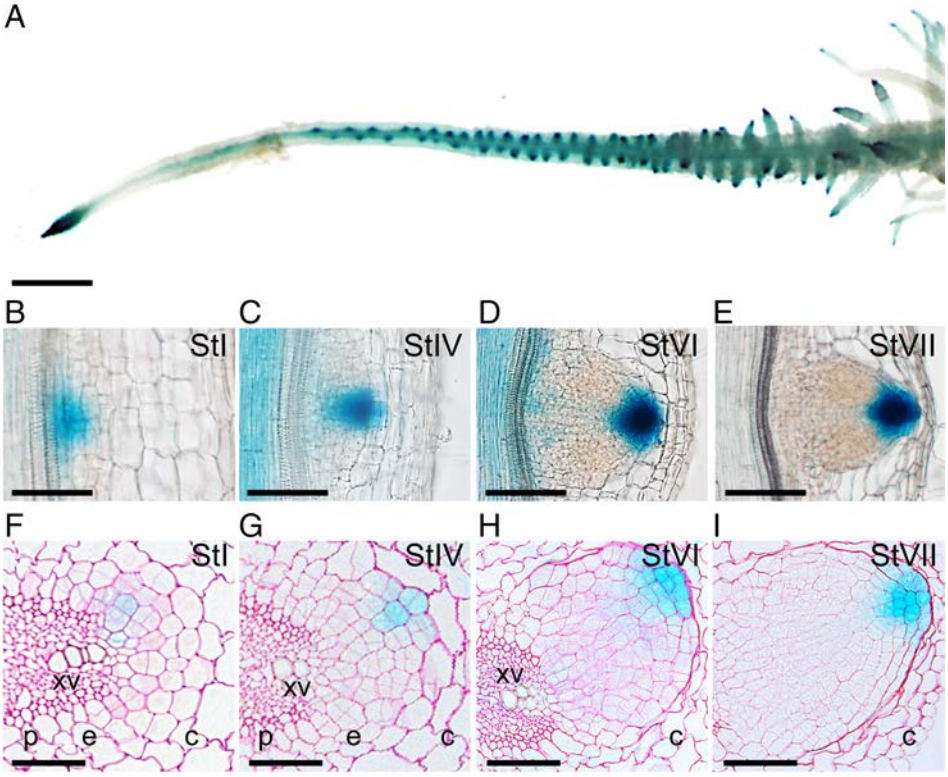

Fig. 3. Establishment of an auxin gradient during CR and rootlet development. (A–I) *DR5:GUS* pattern of expression in lupin 'hairy root' seedlings grown on low-phosphate medium. (A) Fully mature whole CR. (B–E) *DR5:GUS* expression was observed on thick longitudinal sections (80 μm) at stage I (B), stage IV (C), stage VI (D) and stage VII (E). (F–I) *DR5:GUS* expression was also observed on thin cross sections (6 μm) in the juvenile region of the CR counterstained with ruthenium red at corresponding stages: stage I (F), stage IV (G), stage VI (H) and stage VII (I). p, pericycle; e, endodermis; c, cortex; xv, xylem vessels. Scale bars are 100 μm.

of seven tandem repeats of an auxin responsive element isolated from soybean (*Glycine max*), showed a strong conserved pattern compared to other species. Indeed, DR5 expression was seen in the CR tip and vasculature (Fig. 3A and Fig. S1A in File S3, Supporting Information). In rootlet primordium, GUS activity was observed at stage I of development (Fig. 3B), in one of the first dividing cells, close to the protoxylem pole. At stage IV, when divisions give rise to a dome-shaped primordium, GUS activity was observed in a few cells at its tip (Fig. 3C). From this stage onwards, a strong DR5 response builds up in the primordium apex (Fig. 3C–E, G–I). After emergence, strong GUS activity was detected in the root cap whereas the zone above the rootlet tip was displaying a weak GUS activity (Fig. S1B–D in File S3). Expression in the vasculature was observed in mature rootlets (Fig. S1C, D in File S3). Our observations of the *DR5:GUS* reporter suggest that an auxin gradient is established during rootlet initiation up to their emergence and maintained during their later development.

Time course analysis of key auxin signalling genes during rootlet development

In order to identify key auxin signalling genes potentially involved in rootlet development, we performed in silico analysis of the available transcriptomic data in white lupin (Secco et al. 2014). In that study, transcriptomic data were produced from three parts of CRs (tip of CR, physiologically immature CR and mature CR) as well as two parts of regular LRs (tip of the LR and mature LR). We identified several auxin-related genes in this dataset encompassing *ARFs*, *Aux/IAAs*, *TIRs*, *PINs*, *AUX-LAXs* and we shortlisted eight genes (Table S1 in File S3) that showed consistent results with BLAST (i.e. for which the cDNA sequence matched the expected orthologous sequences from other species and showed a similar overall gene structure) and for which we managed to amplify fragments by qPCR.

The available transcriptomic dataset (Secco et al. 2014) study represents an important tool for cDNA discovery but we wanted to study gene expression level with a higher resolution than the existing data. Therefore, we developed a sampling method to describe rootlet development along a time course. Our analysis of white lupin root system allowed us to locate the first cluster of rootlets on the CR and perform a temporal sampling covering the different phases of rootlet emergence. We measured the distance to primary root that we defined as the distance between the primary root and the first cluster of rootlets (Fig. S2A in File S3). We sampled 1 cm of CR at a distance of 1 cm from the primary root from 7 days after germination every 12 h for 5 days, therefore we were able to cover the entire rootlet developmental

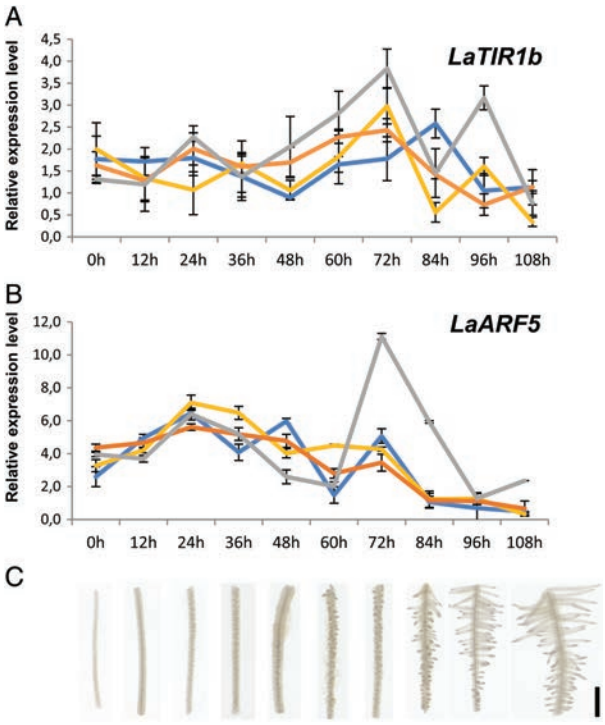

Fig. 4. Relative expression levels of *LaTIR1b* and *LaARF5* during rootlet development. Expression levels of *LaTIR1b* (A) and *LaARF5* (B) are relative to the first time point (0 h) and normalised to *LaUBQ*. Data are mean ± SD of eight CRs coming from four lupin plants (n = 8) with four technical replicates each. Four biological replicates are shown in different colours. (C) 1 cm CR samples collected 1 cm away from the primary root every 12 h were used to assess transcript level during CR development. Scale bar is 0.25 cm.

process. Indeed, 55% of CRs initiate at 1 or 1.5 cm from the primary root and the sampled zone therefore comprises 77% of the produced rootlets (Fig. S3B in File S3). Samples were collected for total RNA extraction and subsequent qRT-PCR analysis (Fig. 4A, B) and imaging (Fig. 4C). We observed that rootlet initiation occurred at 12 h after the first sampling (has) and that rootlet emergence occurred at 72 has (Fig. 4C).

Expression analysis of the eight auxin-related genes showed various overall behaviours during rootlet development (Fig. 4 and Fig. S3 in File S3). Some genes did not show a clear induction or repression response but varied along the time course such as *LaTIR1a* and *LaARF14b*. Others showed a general repression such as *LaARF5*, *LaIAA28* and *LaARF14a* (although for this gene one biological replicate strongly differs from the other three). Two genes showed a peak of induction at around 72 has, such as *LaPIN1* or *LaLAX3,* but not all biological replicates showed matching patterns. Interestingly, *LaTIR1b* showed a general induction during the time course. We decided to focus our attention on two genes: La*TIR1b* and *LaARF5* as shown in Fig. 4A, B. *TIR1* codes for a protein that is part of the SCF/TIR complex, which promotes Aux/IAA protein degradation when auxin is present; and *ARF5* is known to play a role in the very early stages of LR development ensuring the identity of the founder cells (De Smet et al. 2010). Interestingly, *LaTIR1b* is slightly induced during our time course with a peak of expression at 72 has (Fig. 4A). This coincides with the emergence stage. On the opposite, *LaARF5* is repressed during rootlet formation (Fig. 4B), which may suggest a negative control by auxin accumulation in the rootlet primordium.

LaTIR1b and *LaARF5* expressions are altered during rootlet development

We aligned the cDNA-deduced protein sequence of *LaTIR1b* and *LaARF5* with their orthologous genes from *A. thaliana* and generated phylogenetic trees (Fig. 5A and Fig. S4 in File S3). LaTIR1b appeared to be the closest orthologue of AtTIR1 with 77% identity at the entire protein level, suggesting that the automatic annotation was fairly accurate (Fig. 5A). However, LaARF5 groups in a branch that contains three close orthologues: AtARF11, AtARF18 and AtARF9. LaARF5 highest identity level is with AtARF11 at 70% whereas its shares only 50% identity with AtARF5 suggesting that this gene annotation is not very accurate (Fig. S4 in File S3). Furthermore, LaARF5 is predicted to act as a repressor-like AtARF11 and not as an activator-like AtARF5.

To characterise the expression pattern of these two genes, we used an ISGW approach to identify the promoter regions of *LaTIR1b* and *LaARF5* (see the Section 2). These promoters were amplified from genomic DNA and subsequently cloned and sequenced to validate their nucleotide sequence. We then analysed the promoter region of the two genes using the SOGO database (Higo et al. 1999), which revealed numerous potential binding sites for various transcription factors among which some are hormone related (Table S2 in File S3) and thus potentially important in the context of rootlet development. The position of these binding sites in the promoter of each gene is indicated in Figs 5B and 6A. The promoters of *LaTIR1b* (Fig. 5B) and *LaARF5* (Fig. 6A) contain a canonical AuxRE that is known to be a target site for ARF transcription factors. They also contain several Arabidopsis response regulator sites that are present in the promoter of cytokinin-induced genes (three for *LaTIR1b* and four for *LaARF5*). The promoter of *LaARF5* contains a gibberellin-related binding site and two sites found in small auxin upregulated RNA genes, these sites were not found in the promoter of *LaTIR1b*.

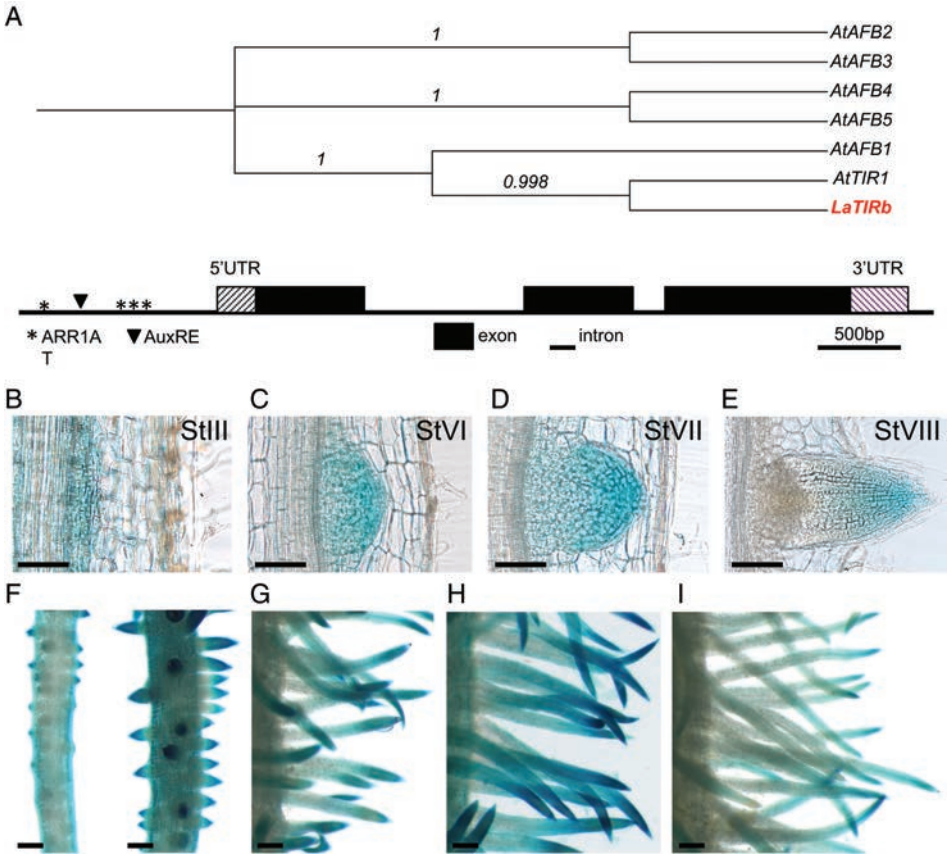

Fig. 5. Genetic study and expression pattern of *LaTIR1b,* a lupin orthologue of Arabidopsis *TIR1*. (A) Neighbour joining tree showing relationship of *LaTIR1b* with *AtTIR/AFB* from *Arabidopsis thaliana*. *LaTIR1b* gene structure seems to be closely related to *AtTIR1*. The bootstrap consensus tree was inferred from 500 replicates. Branches corresponding to partitions reproduced in less than 50% bootstrap replicates were collapsed. (B) Gene structure of *LaTIR1b*. Hormone-related *cis*-acting regulatory elements, exons, introns and position of 5′UTR and 3′UTR are shown (graph to scale). (C–K) Expression pattern of *pLaTIR1b:GUS* in 4-week-old plants grown in low phosphate conditions. GUS activity was found in developing primordia of rootlets at stage III (C), stage VI (D), stage VII (E), stage VIII (F) and appeared homogeneous along the cluster at early (G) and late stages (H) of rootlet formation. Later on, expression showed a clear gradient with stronger activity at the rootlet tip at three stages of rootlet development: young rootlets (I), middle-aged rootlets (J) and old rootlets (K). Scale bars are 100 μm (C–F) and 0.5 mm (G–K).

In order to further characterise the expression pattern governed by these promoters, we fused them to the ß-glucuronidase coding region to create *pLaTIR1b:GUS* and *pLaARF5:GUS* expression vectors. These vectors were transfected into *A. rhizogenes* and used to genetically transform white lupin plants by 'hairy root' (Uhde-Stone et al. 2005). We examined *pLaTIR1b:GUS* expression during the development of rootlets. In developing primordia, *pLaTIR1b* was first expressed at stage III (Fig. 5C) and a slight expression gradient was visible at the apex primordia in the following developmental stages (Fig. 5D–F). In the rootlet, a very strong gradient of expression was observed in young and middle-aged rootlets (Fig. 5G–J) and a maximum of expression remained in the rootlet tip, corresponding to the meristem and elongation zone (Fig. 5I, J). In the rootlet, *LaTIR1b* was expressed in the vasculature throughout their lifetime and expression at the rootlet tip faded away in older rootlets (Fig. 5K).

We also examined *pLaARF5:GUS* expression during rootlet development. Our analysis revealed that p*LaARF5* is expressed in the CR vasculature but its expression is absent from the rootlet primordium. No GUS coloration was found from early stage up to after emergence (Fig. 6B–E). Furthermore, *pLaARF5:GUS* expression in the surrounding tissues weakened during the growth of the rootlet primordium (Fig. 6F, G), which is consistent with the global repression of *LaARF5* found in our qRT-PCR analysis (Fig. 4B). At later rootlet development, expression in the vasculature could be detected, mimicking the expression profile in the CR (Fig. 6J).

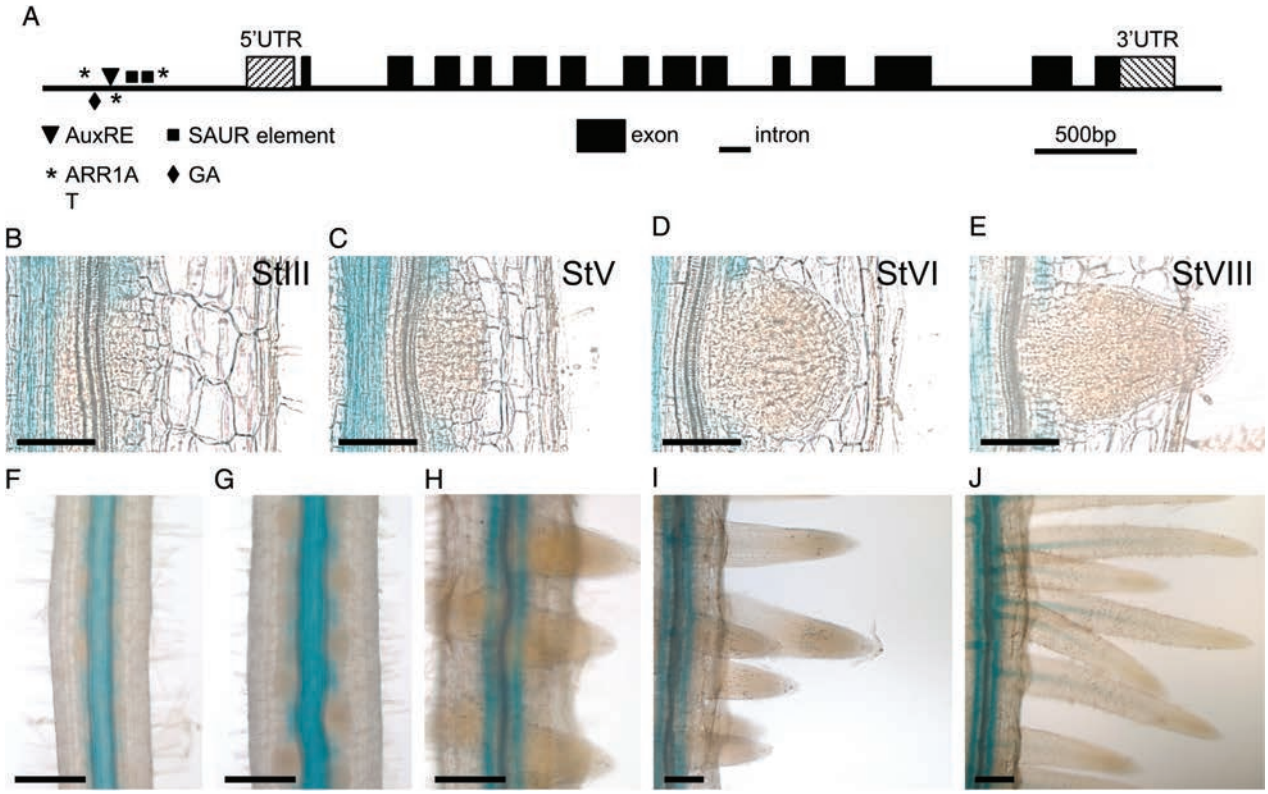

Fig. 6. Genetic study and expression pattern of *LaARF5,* a lupin orthologue of *Arabidopsis thaliana ARF11*. (A) Gene structure of *LaARF5*. Hormone-related *cis*-acting regulatory elements (as defined in Table S2 in File S3), exons, introns and position of 5′UTR and 3′UTR are shown (graph to scale). (B–J) Expression pattern of *pLaARF5:GUS* in 4-week-old plants grown in low phosphate conditions. GUS activity was absent in developing primordia of rootlets at stage III (B), stage V (C), stage VI (D), stage VIII (E) and remained in the CR vasculature (F), absent from early (G) and late stages of rootlet emergence (H) and mature rootlet (I). Expression resumed in the vasculature in old rootlets (J). Scale bars are 100 μm (B–E) and 200 μm (F–J).

Discussion

Previous work on white lupin CR has been largely focussed on its physiology because it is a very active organ with high levels of exudation involved in the root phosphate acquisition (Neumann 2000, Massonneau et al. 2001, Yan et al. 2002, Hocking and Jeffery 2004). In this study, we decided to focus on CR because of its atypical mode of development, corresponding to the production of numerous rootlets initiated in a synchronous manner and with a limited lifetime. Our approach has revealed that the early divisions of rootlets are very similar to what is observed in other species LR development, like the model plant Arabidopsis or even in legumes. Indeed, LR development in these species is initiated by divisions in the pericycle cells in front of the xylem poles (Dubrovsky et al. 2000), and this is the case for white lupin rootlets (Fig. 2). Cellular division in the endodermis and cortex are regularly observed in legume species – like *Medicago truncatula* (Herrbach et al. 2014) – but not in Arabidopsis, this may be linked with the presence of numerous cortical cell layers and with the comparatively important size of the primordia. We provide here a detailed anatomical description of the various stages of rootlet development along the CR that will prove useful in the future to characterise mutants or genetically altered plants but also to deepen the study of the molecular mechanisms regulating CR development.

In parallel, we have set up an original sampling procedure that covers the entire development process, from the rootlet initiation to the rootlet senescence, and this system allows for the description of gene expression profiling during rootlet development, even if some discrepancies are observed probably due to plant to plant genetic variability. We focussed here on describing some auxin-related gene expressions and we identified two genes with contrasted expression profiles (Fig. 4). Further analysis of their expression pattern at the tissular level confirmed the induction and repression of *LaTIR1b* and *LaARF5,* respectively (Figs 5 and 6), and validated our time course sampling method. *LaARF5* was previously annotated based on RNAseq assembly in the absence of a reference genome for white lupin (Secco

et al. 2014). However, phylogeny analysis revealed that it is the closest orthologue to *AtARF11*. In accordance, *LaARF5* and *AtARF11* are both predicted to be repressor ARFs whereas *AtARF5* is an activator. Furthermore, *AtARF5/MONOPTEROS* is expressed in LR primordium from as early as stage I and up to emergence (De Smet et al. 2010, Ckurshumova et al. 2014) whereas *LaARF5* is not expressed in CR primordia (Fig. 6). Further work will be needed to understand how these two genes are regulated, including by hormonal signals, and how they fit in larger gene regulatory networks. Whole-genome transcriptional studies are an essential step to finely identify new genes regulating LR development and the CR model seems to be perfectly adapted to this strategy.

Another key feature of rootlet development is that they all enter into senescence simultaneously. In fact, rootlet meristems are determinate, meaning that they stop dividing and undergo full differentiation up to their tip (Watt and Evans 1999). This mode of growth is directly related to the function of the CR and to the chemical nature of phosphate. Indeed, inorganic phosphate is poorly mobile in the soil, therefore CRs are able to remobilise as much phosphate as possible and subsequently uptake it for the plant nutrition (Hinsinger et al. 2011). However, soil phosphate patches are quickly used up and new clusters are produced in a distant site to forage for more phosphate. As a result, CRs are ephemeral structures by nature due to rootlets determinacy. In laboratory conditions (hydroponic culture medium), we expose roots systems to a permanent and homogeneous lack of phosphate. In these conditions, rootlets are produced, grow to their mature length and then stop growing demonstrating that there is no need for a feedback from the medium to control their growth behaviour. This raises several important questions regarding the order of events leading to rootlet growth arrest: when does cell elongation and division stop? Is the determinacy of the meristem already established in the rootlet primordium? Does the primordium ever acquire a meristematic organisation? Does a maximum of auxin form in the rootlet meristem? Here, the use of the DR5 marker allowed us to confirm the establishment of such a maximum of auxin that seems to be maintained throughout the course of rootlet development up to its mature length (Fig. 3 and Fig. S1 in File S3). More work will be needed to describe precisely how rootlet determinacy is genetically controlled and if a mechanism similar to what is known about Arabidopsis primary root development can be described (Balzergue et al. 2017). In this regard, studying the establishment of a quiescent centre and its maintenance during rootlet growth could be of great interest.

With regards to root developmental adaptations, white lupin is a fantastic model to parallel with other models like Arabidopsis or *M. truncatula* for a better understanding of the mechanisms regulating the development of LRs but many genomic tools are still missing to conduct further analysis. We believe that future work will produce these tools and help understand how CR development is tightly controlled to produce such amazing structures.

Acknowledgements – This project has received funding from the European Research Council under the European Union's Horizon 2020 research and innovation program (Starting Grant Lupin Roots – grant agreement No 637420 to B. P.). C. G. is the recipient of a fellowship from GAIA doctoral school of Montpellier University. We acknowledge the help of the imaging facility MRI, member of the national infrastructure France-BioImaging supported by the French National Research Agency (ANR-10-INBS-04, «Investments for the future».

References

Abdolzadeh A, Wang X, Veneklaas EJ, Lambers H (2010) Effects of phosphorus supply on growth, phosphate concentration and cluster-root formation in three Lupinus species. Ann Bot 105: 365–374

Balzergue C, Dartevelle T, Godon C, Laugier E, Meisrimler C, Teulon JM, Creff A, Bissler M, Brouchoud C, Hagège A, Müller J, Chiarenza S, Javot H, Becuwe-Linka N, David P, Péret B, Delannoy E, Thibaud MC, Armengaud J, Abel S, Pellequer JL, Nussaume L, Desnos T (2017) Low phosphate activates STOP1-ALMT1 to rapidly inhibit root cell elongation. Nat Commun 8: 15300

Benková E, Michniewicz M, Sauer M, Teichmann T, Seifertová D, Jürgens G, Friml J (2003) Local, efflux-dependent auxin gradients as a common module for plant organ formation. Cell 115: 591–602

Billou I, Xu J, Wildwater M, Willemsen V, Paponov I, Friml J, Heldstra R, Aida M, Palme K, Scheres B (2005) The PIN auxin efflux facilitator network controls growth and patterning in Arabidopsis roots. Nature 433: 39–44

Casimiro I, Beeckman T, Graham N, Bhalerao R, Zhang H, Casero P, Sandberg G, Bennett MJ (2003) Dissecting Arabidopsis lateral root development. Trends Plant Sci 8: 165–171

Ckurshumova W, Smirnova T, Marcos D, Zayed Y, Berleth T (2014) Irrepressible MONOPTEROS/ARF5 promotes de novo shoot formation. New Phytol 204: 556–566

Cu STT, Hutson J, Schuller KA (2005) Mixed culture of wheat (Triticum aestivum L.) with white lupin (*Lupinus albus* L.) improves the growth and phosphorus nutrition of the wheat. Plant and Soil 272: 143–151

De Rybel B, Vassileva V, Parizot B, Demeulenaere M, Grunewald W, Audenaert D, Van Campenhout J, Overvoorde P, Jansen L, Vanneste S, Möller B, Wilson M, Holman T, Van Isterdael G, Brunoud G, Vuylsteke M,

Vernoux T, De Veylder L, Inzé D, Weijers D, Bennett MJ, Beeckman T (2010) A novel aux/IAA28 signaling cascade activates GATA23-dependent specification of lateral root founder cell identity. Curr Biol 20: 1697–1706

De Smet I, Lau S, Voß U, Vanneste S, Benjamins R, Rademacher EH, Schlereth A, De Rybel B, Vassileva V, Grunewald W, Naudts M, Levesque MP, Ehrismann JS, Inze D, Luschnig C, Benfey PN, Weijers D, Van Montagu MCE, Bennett MJ, Jürgens G, Beeckman T (2010) Bimodular auxin response controls organogenesis in Arabidopsis. Proc Natl Acad Sci USA 107: 2705–2710

Dharmasiri N, Dharmasiri S, Estelle M (2005) The Arabidopsis F-box protein TIR1 is an auxin receptor. Nature 435: 441–445

Du Y, Scheres B (2017) Lateral root formation and the multiple roles of auxin. J Exp Bot 69: 155–167

Dubrovsky JG, Doerner PW, Colón-Carmona a RTL (2000) Pericycle cell proliferation and lateral root initiation in Arabidopsis. Plant Physiol 124: 1648–1657

Dubrovsky JG, Sauer M, Napsucialy-Mendivil S, Ivanchenko MG, Friml J, Shishkova S, Celenza J, Benková E (2008) Auxin acts as a local morphogenetic trigger to specify lateral root founder cells. Proc Natl Acad Sci USA 105: 8790–8794

Fukaki H, Tasaka M (2009) Hormone interactions during lateral root formation. Plant Mol Biol 69: 437–449

Hagström J, James WM, Skene KR (2001) A comparison of structure, development and function in cluster roots of *Lupinus albus* L. under phosphate and iron stress. Plant and Soil 232: 81–90

Herrbach V, Remblière C, Gough C, Bensmihen S (2014) Lateral root formation and patterning in Medicago truncatula. J Plant Physiol 171: 301–310

Higo K, Ugawa Y, Imamoto M, Korenaga T (1999) Plant cis-acting regulatory DNA elements (PLACE) database. Nucleic Acids Res 27: 297–300

Hinsinger P, Brauman A, Devau N, Gérard F, Jourdan C, Laclau JP, Le Cadre E, Jaillard B, Plassard C (2011) Acquisition of phosphorus and other poorly mobile nutrients by roots. Where do plant nutrition models fail? Plant and Soil 348: 29–61

Hocking PJ, Jeffery S (2004) Cluster-root production and organic anion exudation in a group of old-world lupins and a new-world lupin. Plant and Soil 258: 135–150

Huang X, Madan A (1999) A DNA sequence assembly program. Genome Res 9: 868–877

Karimi M, Inze D, Depicker A (2002) GATEWAY vectors for agrobacterium-mediated plant transformation. Trends Plant Sci 7: 193–195

Kepinski S, Leyser O (2005) The Arabidopsis F-box protein TIR1 is an auxin receptor. Nature 435: 446–451

Kurihara D, Mizuta Y, Sato Y, Higashiyama T (2015) ClearSee: a rapid optical clearing reagent for whole-plant fluorescence imaging. Development 142: 4168–4179

Lambers H, Teste FP (2013) Interactions between arbuscular mycorrhizal and non-mycorrhizal plants: do non-mycorrhizal species at both extremes of nutrient availability play the same game? Plant Cell Environ 36: 1911–1915

Lambers H, Finnegan PM, Jost R, Plaxton WC, Shane MW, Stitt M (2015) Phosphorus nutrition in Proteaceae and beyond. Nat Plants 1: 1–9

Laplaze L, Benková E, Casimiro I, Maes L, Vanneste S, Swarup R, Weijers D, Calvo V, Parizot B, Herrera-Rodriguez MB, Offringa R, Graham N, Doumas P, Friml J, Bogusz D, Beeckman T, Bennett M (2007) Cytokinins act directly on lateral root founder cells to inhibit root initiation. Plant Cell Online 19: 3889–3900

Laskowski M, Biller S, Stanley K, Kajstura T, Prusty R (2006) Expression profiling of auxin-treated Arabidopsis roots: toward a molecular analysis of lateral root emergence. Plant Cell Physiol 47: 788–792

Lavenus J, Goh T, Roberts I, Guyomarc'h S, Lucas M, De Smet I, Fukaki H, Beeckman T, Bennett M, Laplaze L (2013) Lateral root development in Arabidopsis: fifty shades of auxin. Trends Plant Sci 18: 1360–1385

Livak KJ, Schmittgen TD (2001) Analysis of relative gene expression data using real-time quantitative PCR and the $2^{-\Delta\Delta CT}$ method. Methods 25: 402–408

Malamy JE, Benfey PN (1997) Organization and cell differentiation in lateral roots of *Arabidopsis thaliana*. Development 124: 33–44

Massonneau A, Langlade N, Léon S, Smutny J, Vogt E, Neumann G, Martinoia E (2001) Metabolic changes associated with cluster root development in white lupin (*Lupinus albus* L.): relationship between organic acid excretion, sucrose metabolism and energy status. Planta 213: 534–542

Meng ZB, Chen LQ, Suo D, Li GX, Tang CX, Zheng SJ (2012) Nitric oxide is the shared signalling molecule in phosphorus- and iron-deficiency-induced formation of cluster roots in white lupin (*Lupinus albus*). Ann Bot 109: 1055–1064

Meng ZB, You XD, Suo D, Chen YL, Tang C, Yang JL, Zheng SJ (2013) Root-derived auxin contributes to the phosphorus-deficiency-induced cluster-root formation in white lupin (*Lupinus albus*). Physiol Plant 148: 481–489

Moreno-Risueno MA, Van Norman JM, Moreno A, Zhang J, Ahnert SE, Benfey PN (2010) Oscillating gene expression determines competence for periodic Arabidopsis root branching. Science 329: 1306–1311

Neumann G (2000) Physiological aspects of cluster root function and development in phosphorus-deficient white lupin (*Lupinus albus* L.). Ann Bot 85: 909–919

Péret B, De Rybel B, Casimiro I, Benková E, Swarup R, Laplaze L, Beeckman T, Bennett MJ (2009) Arabidopsis

lateral root development: an emerging story. Trends Plant Sci 14: 399–408
Secco D, Shou H, Whelan J, Berkowitz O (2014) RNA-seq analysis identifies an intricate regulatory network controlling cluster root development in white lupin. BMC Genom 15: 230
Shane MW, Lambers H (2005) Cluster roots: a curiosity in context. Plant and Soil 274: 101–125
Skene KR (2000) Pattern formation in cluster roots: some developmental and evolutionary considerations. Ann Bot 85: 901–908
Uhde-Stone C, Liu J, Zinn KE, Allan DL, Vance CP (2005) Transgenic proteoid roots of white lupin: a vehicle for characterizing and silencing root genes involved in adaptation to P stress. Plant J 44: 840–853
Ulmasov T, Murfett J, Hagen G, Guilfoyle TJ (1997) Aux/IAA proteins repress expression of reporter genes containing natural and highly active synthetic auxin response elements. Plant Cell 9: 1963–1971
Ulmasov T, Hagen G, Guilfoyle TJ (1999) Dimerization and DNA binding of auxin response factors. Plant J 19: 309–319
Untergasser A, Cutcutache I, Koressaar T, Ye J, Faircloth BC, Remm M, Rozen SG (2012) Primer3-new capabilities and interfaces. Nucleic Acids Res 40: 1–12
Vance CP, Uhde-Stone C, Allan DL (2003) Phosphorus aquisition and use: critical adaptations by plants for securing a nonrewable resource. New Phytol 157: 423–447
Von Wangenheim D, Fangerau J, Schmitz A, Smith RS, Leitte H, Stelzer EHK, Maizel A (2016) Rules and self-organizing properties of post-embryonic plant organ cell division patterns. Curr Biol 26: 439–449
Wang Z, Straub D, Yang H, Kania A, Shen J, Ludewig U, Neumann G (2014) The regulatory network of cluster-root function and development in phosphate-deficient white lupin (*Lupinus albus*) identified by transcriptome sequencing. Physiol Plant 151: 323–338
Wang Z, Rahman ABMM, Wang G, Ludewig U, Shen J, Neumann G (2015) Hormonal interactions during cluster-root development in phosphate-deficient white lupin (*Lupinus albus* L.). J Plant Physiol 177: 74–82
Watt M, Evans J (1999) Linking development and determinacy with organic acid efflux from proteoid roots of white lupin grown with low phosphorus and ambient or elevated atmospheric CO_2 concentration. Plant Physiol 120: 705–716
Xuan W, Audenaert D, Parizot B, Möller BK, Njo MF, De Rybel B, De Rop G, Van Isterdael G, Mähönen AP, Vanneste S, Beeckman T (2015) Root cap-derived auxin pre-patterns the longitudinal axis of the Arabidopsis root. Curr Biol 25: 1381–1388
Yan F, Zhu Y, Mu C, Zo C, Schubert S (2002) Adaptation of H-pumping and plasma membrane H ATPase activity in proteoid roots of white lupin under phosphate deficiency 1. Plant Physiol 129: 50–63

Supporting Information

Additional supporting information may be found online in the Supporting Information section at the end of the article.

File S1. Full genomic sequence of LaTIR1b with UTR and exon/intron annotation.

File S2. Full genomic sequence of LaARF5 with UTR and exon/intron annotation.

File S3. Supporting Information.

Fig. S1. *DR5:GUS* expression pattern in white lupin CR.

Fig. S2. Distance to primary root of the first cluster of rootlets is a robust trait.

Fig. S3. Relative level of expression of six auxin-related genes during CR development.

Fig. S4. Neighbour joining tree showing relationship of *LaARF5* with ARFs from *Arabidopsis thaliana*.

Table S1. Shortlist of auxin-related genes identified in white lupin.

Table S2. List of hormone-related *cis*-acting elements identified in *LaTIR1b* and *LaARF5* promoters.

Edited by K. Ljung